Role of lone-pair interactions and local disorder in determining the interdependency of optical constants of *a*-CN:H thin films

G. Fanchini,[1] A. Tagliaferro,[1] N. M. J. Conway,[2,*] and C. Godet[2]
[1]*Dipartimento di Fisica and Unità INFM, Politecnico di Torino, I-10129 Torino, Italy*
[2]*LPICM, UMR 7647-CNRS, Ecole Polytechnique, 91128 Palaiseau Cedex, France*
(Received 2 April 2002; published 27 November 2002)

In this paper the role of the nitrogen bonding regime and of the presence of lone-pair electrons due to nitrogen atoms on the optical properties of disordered hydrogenated carbon nitride (*a*-CN:H) thin films grown by reactive sputtering are studied. Evidence is given for the existence of a variable amount of mixing between nitrogen atom lone-pair states and π bonding electronic states in different samples. It is proved that such mixing favors the stabilization of lone pairs. By properly analyzing the role of the local disorder and of the lone-pair π mixing, an ellipsometric model able to describe the optical complex dielectric constant, measured in the UV-visible range, is developed. The existence of an optical scaling law for the real and imaginary parts of the dielectric function is demonstrated.

DOI: 10.1103/PhysRevB.66.195415 PACS number(s): 78.66.−w, 73.22.−f, 78.20.Ci, 78.30.Ly

I. INTRODUCTION

The considerable interest in carbon nitride-based thin films (see Refs. 1–3) is usually justified by the wide range of mechanical applications that the synthesis of the theoretically predicted superhard C_3N_4 phases could open. Nowadays, while most of the effort in growing even small C_3N_4 crystallites seems to be quite far from the goal,[1] other applications of carbon nitrides are attracting interest. Such applications sometimes require very different growing processes and nitrogen contents with respect to those currently considered to prepare the superhard phases. For instance, the addition of a few nitrogen atoms inside *a*-C:H-based materials is shown to improve some electronic properties such as their photoluminescence,[4] electroluminescence,[3] and field-emission[5] properties. Very small amounts of nitrogen atoms cause the disordered carbon-based materials (either tetrahedral or graphitelike) to become *n* type.[6] The main contribution to such an effect seems related to the nucleation of the carbon sp^2 phase[7] around nitrogenated sites (that can be either sp^2- or sp^1-hybridized). Moreover, at least for optical applications, soft and low coordinated (polymerlike) materials appear more attractive than the hardest and densest ones. The hydrogen addition during deposition could improve their properties by increasing the number of terminal bonds and producing a more relaxed structure. In the perspective of such applications, the film characterization should focus more on the electronic states. This is a problematic point since, even in non-nitrogenated amorphous carbon materials though the gross features of the electronic structure are understood, only a small amount of detailed quantitative information is available. In addition, the ability of nitrogen to cluster with the sp^2- (and/or sp^1-) hybridized carbon atoms and to contribute to the π-states amount complicates the electronic picture. Optical and electronic properties of all the disordered carbon-based materials in the visible-near-ultraviolet (VIS-NUV) energy range are in fact largely determined by π and π^* states.

The aim of the present paper is to study the effects of nitrogen incorporation on the properties of *a*-CN:H materials. The nitrogen lone-pair interactions with π states belonging to neighboring C and N atoms and the local disorder are taken into account and the consequent site-to-site fluctuations of the nonbonding level considered. The role of such phenomena in determining the optical properties of a set of reactively sputtered *a*-CN:H materials and the existence of a scaling law for the optical properties of such *a*-CN:H films are demonstrated.

II. EXPERIMENT

Samples were deposited in a conventional rf (13.56 MHz) diode sputtering system.[8] The carbon ions sputtered from the graphite cathode (99.999% purity) mix with the chamber $Ar+He+N_2+H_2$ reactive atmosphere. No external bias voltage was applied at the substrate. The He/Ar flow-rate ratio (3/7) and substrate temperature (100 °C) were kept fixed. No more than one parameter (rf power, chamber pressure, gas flow rates. etc) was varied from one deposition to the other (Table I). One additional sample (sample 1) was prepared under conditions known to produce sp^2-rich and electrically conductive materials. Nitrogen content was evaluated by Rutherford backscattering and nuclear reaction analysis with a relative uncertainty ~30%. H content was evaluated by elastic recoil detection analysis. The N content of the films is always close to 10%, while the H content ranges from 14% (sample 2) to 20% (sample 7). Such compositions refer to the total N and H contents (irrespective of the bonded or free nature of the atoms). Preliminary results of small-angle x-ray scattering analyses performed on samples deposited under similar conditions show the films to be amorphous or, at least, containing sp^2 clusters below the minimum detectable size [estimated around 12–15 Å (Ref. 9)]. The samples were optically characterized by *ex situ* UV-visible spectroscopic phase-modulated ellipsometry in the 1.5–5 eV photon energy range using a Jobin-Yvon UVISEL system. The measured spectra were fitted using the Tauc-Lorentz[10] model to obtain refractive indices (n) and

TABLE I. Deposition conditions.

Sample	1	2	3	4	5	6	7
rf power (W)	220	300	400	300	300	300	300
p_{tot} (mTorr)	38	25	20	20	20	20	20
F_{N_2} (SCCM)	4	10	10	7	10	10	20
F_{H_2} (SCCM)	3	7	5	5	7	7	7
F_{Ar} (SCCM)	30	70	70	70	70	70	70
F_{He} (SCCM)	70	30	30	30	30	30	30
Self-bias voltage (V)	−350	−890	−1000	−890	−890	−890	−890
Thickness (nm)	250	370	460	520	440	370	300

extinction coefficients (k), as well as the complex dielectric functions ($\varepsilon_1 + i\varepsilon_2$) and the film thickness.

III. THE ROLES OF NITROGEN AND DISORDER

In the VIS-NUV range, the optical transitions are governed by the π and π^* electronic state distributions, related to sp^2- and sp^1-hybridized C and N atoms. Specific lone-pair electronic states arise from groups (CN) with sp^1-hybridized C atoms, which may form C≡N triple bonds or —N═C═N— longer chains, as observed previously in sputtered films.[11] In the following, we will discuss the role of nitrogen and local disorder in determining the nature and energy distribution of the electronic states. In particular, we will show how the modifications of the π-π^* transitions due to N lone pairs and local fluctuation effects can be incorporated in the optical modeling.

A. Lone-pair π mixing and partial delocalization of the lone-pair electrons

sp^1- and sp^2-hybridized nitrogen atoms have unshared highly localized σ-electron lone pairs that, even if stabilized by the local environment, are energetically located closer to midgap than the σ-bonded states of the C-C, C-N, C-H, or N-H bonds.[1] Interactions between the lone-pair (LP) and π states of the carbon nitride matrix may result from ''orbital-mixing'' effects. The term mixing may involve different physical effects that are hardly separable and can be treated in the same way in the framework of our model:

(i) the LP interaction with the other *atomic* orbitals of the N atom, likely prevailing in constrained carbon nitride structures, and

(ii) the LP interaction with the *molecular* π orbitals formed by the clustered C and/or N atoms surrounding the lone pair, dominant in floppy materials. This interaction involves a partial conjugation of the original p and LP states, leading to an increase in the spatial extension of the ''mixed'' LP states as compared to noninteracting LP states. Such a mixing is expected to prevail in the low-density, H-rich carbon nitride films examined in this paper.

While the first type of ''mixing'' is connected with distortions, the second type is due to the fact that lone pairs and π states are sitting on different ions. Hence, as LP states have s character and spherical symmetry, they can mix with π orbitals sitting on nearby ions.

B. The density of electronic states and the disorder-broadening effects

In unalloyed a-C:H as a consequence of the overlap between nearest-neighboring p-atomic orbitals, π bands are narrower and closer to the local nonbonding level with respect to π^* bands.[12] The bonding and antibonding density-of-states (DOS) distributions in carbon nitride alloys are expected to be strongly affected by the mixing effects. As a consequence of the localized nature of the states, the definition of an overall Fermi level for the sp^2 phase is not possible. Larger Gaussian widths for the bonding DOS can then be attributed to the shifts of the local (nonpinned) nonbonding energy level needed in order to maximize the local bonding energy. Such a shift is strongly dependent on the increased number of loosely bonded electrons provided by nitrogen atoms, which can participate in the LP-π mixing. In the presence of relevant nitrogen alloying effects, the overlap between nearest-neighboring p-atomic orbitals[12] becomes a secondary source of asymmetry with respect to the aforementioned broadening of the bonding DOS and the subsequent nonbonding level shift. A (LP-π mixed) bonding state can even sit farther from the local nonbonding level than the corresponding antibonding one. Hence, the DOS model contemplating asymmetries between the bonding and antibonding DOS in a-C:H (Ref. 12) still holds for a-CN:H (Fig. 1) though the asymmetries may have different physical origin.

A Gaussian-like shape and a scaling relationship between peak position and peak width have been demonstrated for π and π^* bands[13] as a consequence of the fluctuation of the local disorder. The CN groups relevant to the LP-π mixing are located close to (or inside) sp^2 clusters, and consequently affected by the same amount of disorder affecting the C sp^2 sites. In addition, sp^3 and sp^1 phases are unable to coexist under thermodynamic equilibrium conditions[14] and our deposition process is not expected to largely depart from such conditions. Hence, LP states should also be described by a Gaussian-shaped DOS, characterized by a peak position E_{LP} and a width σ_{LP}, and we expect the same scaling relationship between peak position and peak width to hold for π (and π^*) and LP bands. Let us assume the Gaussian-shaped

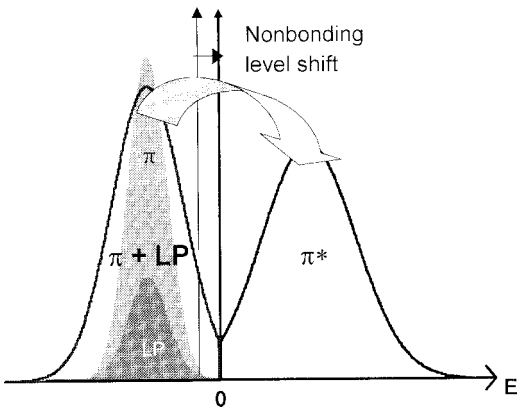

FIG. 1. Schematic of the density of states near the "Fermi level." The effect of LP-π mixing is evidenced by the broadening of the mixed LP+π band with respect to the original "unmixed" LP and π ones. The "nonbonding level shift" consequent to the mixing is sketched.

disorder-broadened bands to be centered at $-E_\pi$, E_{π^*}, and $-E_{\mathrm{LP}}$, respectively. The origin of the energy scale is set at the average nonbonding level. For the sake of simplicity we will assume π and π^* DOS to be symmetric with respect to the origin, and E_π will be equal to E_{π^*}. We perform a *scaling*[13,15] of the peak energies by dividing each peak energy by the correspondent half width at half maximum ($\sigma_\pi = \sigma_{\pi^*}$ and σ_{LP}) so that a quantity W_0 independent of the given film is obtained:

$$E_\pi/\sigma_\pi = E_{\pi^*}/\sigma_{\pi^*} = E_{\mathrm{LP}}/\sigma_{\mathrm{LP}} = W_0 = \text{const.} \tag{1}$$

As outlined in Sec III A, a π and LP mixing effect occurs due to disorder and local distortions. The Appendix shows that, assuming both nonmixed π and LP bands as Gaussian shaped, the DOS arising from their mixing is still Gaussian shaped, peaked between the two LP- and π-states Gaussian, and wider than each of them (see Fig. 1). The parameter

$$V_{\mathrm{N0}} = E_{\mathrm{LP}}/E_\pi = \sigma_{\mathrm{LP}}/\sigma_\pi \tag{2}$$

takes into account the difference in the peak positions of the π and LP DOS. For LP states sitting on the material nonbonding level we have $V_{\mathrm{N0}}=0$ and a δ-shaped LP DOS, while $V_{\mathrm{N0}}=1$ implies that the π and LP DOS are superposed. As a consequence of π-LP mixing, the peak of the π-LP band moves to an intermediate position between E_{LP} and E_π, so that the scaled (by disorder) peak-to-peak energy W_{N0} between the mixed π-LP and the π^* bands is given by (see the Appendix)

$$W_{\mathrm{N0}} = \frac{V_{\mathrm{N0}}+3}{2[2(V_{\mathrm{N0}}^2+2)]^{1/2}} W_0 . \tag{3}$$

It can be observed that (Appendix)

(i) the bonding DOS "band" broadens because of LP-π mixing:

(ii) the "mixed" LP-π DOS band is peaked between the LP and π peaks ($E_{\pi\mathrm{N}} = [E_\pi + E_{\mathrm{LP}}]/2$).

C. The joint density of electronic states (J_{DOS}) and the optical oscillator density

When optical transitions are considered, the relevant quantity affecting the dielectric constant is not the DOS itself, but the so-called J_{DOS}, defined as[16]

$$J_{\mathrm{DOS}}(h\upsilon) = \int_0^{h\upsilon} N_o(Z-h\upsilon) N_u(Z)\, dZ. \tag{4}$$

Assuming the matrix element Q of the transition to be independent of the energy of the initial (occupied) and final (unoccupied) states, the imaginary part of the dielectric constant can be written as[16]

$$\varepsilon_2(h\upsilon) = Q^2 \cdot J_{\mathrm{DOS}}(h\upsilon)/(h\upsilon)^2. \tag{5}$$

In turn, the optical oscillator density will be given by[17]

$$f(E) = \int_0^E (h\upsilon)\varepsilon_2(h\upsilon)\, d(h\upsilon). \tag{6}$$

In order to analyze the optical oscillator density at a given photon energy we hypothesize in our case that in addition to absorption processes due to $\pi \rightarrow \pi^*$ transitions, other transitions related to the presence of nitrogen appear. In particular, $\pi \rightarrow \pi^*$ and LP$\rightarrow \pi^*$ transitions coexist, the contribution of the latter being controlled by the total concentration n_{π^*} of π^* states (that equals the total concentration of π states n_π) and the concentration n_{CN} of CN groups, providing a lone-pair each (i.e., if n nitrogen atoms with a lone pair each are present in the group, they would be counted as n groups). Applying the *f*-sum rule[17] we obtain the oscillator strength density f_{LP} of the LP$\rightarrow \pi^*$ transitions,

$$f_{\mathrm{LP}} \propto (n_{\mathrm{CN}} \cdot n_\pi)^{1/2} = B \cdot (n_{\mathrm{CN}} \cdot n_\pi)^{1/2}. \tag{7}$$

No linear relation *apparently* holds between n_π and f_{LP} as the LP DOS depends on n_{CN} and does not seem to be uniquely related to n_π. However, several effects (detailed in the following) have to be considered before a final statement can be made.

First of all, each sp^1-hybridized atom involves two π electrons, not the single π electron involved by each sp^2 site, and this will alter the n_π value. The presence of sp^1 nitrogen affects the n_π value in an additional way because, as discussed in Ref. 11, CN groups are expected to favor the nucleation of the sp^2 phase around them.

Such effects can be summarized in the following relationship between n_π and the (sp^1) CN group density (n_{CN}):

$$n_\pi = n_\pi^{(0)} + (2+\varphi) n_{\mathrm{CN}}, \tag{8}$$

where $n_\pi^{(0)}$ is the π-electron density of a hypothetical nonnitrogenated "*a*-C:H precursor," and 2 is the number of π electrons belonging to each CN group. The parameter φ takes into account that nitrogen induces the nucleation of the carbon sp^2 phase and, as such, it also indirectly increases the amount of π states. Our model will not be able to provide an *a priori* estimate for φ (that could even differ from sample to sample without limitation to the model applicability).

Generally speaking, Eq. (8) must be modified in the case in which both sp^2- and sp^1-hybridization of nitrogen atoms occurs. However, this simply means substituting the number 2 in Eq. (8) with a properly averaged number. Hence, the following considerations will also hold for all samples having comparable amounts of sp^2- and sp^1-hybridized nitrogen atoms. Since (at least in the present *hydrogenated* samples[11]) no evidence of a relevant amount of sp^2-hybridized nitrogen atoms was obtained, we will focus the following discussion to the sp^1 case [with the use of number 2 in Eq. (8)].

By substituting n_{CN} from Eq. (8) in the *f*-sum rule described by Eq. (7), we obtain

$$f_{LP}=B\cdot n_{\pi}\left(\frac{1}{2+\varphi}\right)^{1/2}\cdot\left(1-\frac{n_{\pi}^{(0)}}{n_{\pi}}\right)^{1/2}. \tag{9a}$$

where B is a constant. As the nitrogen-related increase of the π-state density is expected to be, at least for sufficiently N-rich films, quite relevant, we assume $n_{\pi}/n_{\pi}^{(0)}\gg 1$. Hence

$$f_{LP}\approx B\cdot n_{\pi}\left(\frac{1}{2+\varphi}\right)^{1/2}\cdot\left(1-\frac{n_{\pi}^{(0)}}{2n_{\pi}}\right). \tag{9b}$$

This allows to write f_{LP} as a sum of a positive (larger) and a negative (smaller) term: $f_{LP}\approx f'_{LP}-f''_{LP}$ (no physical meaning being assigned to the negative contribution $-f''_{LP}$):

$$f'_{LP}(Y)=B(Y,W_0)\cdot n_{\pi}\cdot\left(\frac{1}{2+\varphi}\right)^{1/2},$$

$$f''_{LP}(Y)=B(Y,W_0)\cdot n_{\pi}^{(0)}\cdot\left(\frac{1}{8+4\varphi}\right)^{1/2}. \tag{10}$$

As evidenced, the coefficient $B=B(Y,W_0)$ will not depend on the single film properties, but only on the scaled energy Y and the scaled peak energy W_0 (see the Appendix for their definitions).

For a non-nitrogenated material $f_{LP}=0$ [from Eq. (9a), as $n_{\pi}=n_{\pi}^{(0)}$], while in the presence of nitrogen alloying effects $f_{LP}\approx f'_{LP}\gg f''_{LP}$. As f_{LP} on its turn is lower than the $\pi\rightarrow\pi^*$ contribution (f_{π}), we can neglect f''_{LP}, assuming $f_{\pi}+f_{LP}\approx f_{\pi}+f'_{LP}$. This is tantamount to assuming that most of the π states sitting close to the lone pairs are (directly or indirectly) related to nitrogen, rather than to the microstructure of the "*a*-C:H precursor."

D. The scaled photon energy and the optical oscillator density

Let us now discuss the scaled photon energy to analyze the optical oscillator density of our films. In the Appendix it is shown that the scaling of photon energy in the presence of LP-π mixing should be performed in the following way:

$$Y_N(E)=\frac{2}{[2(V_{N0}^2+2)]^{1/2}}Y\leqslant Y, \tag{11}$$

where Y ($=E/[2\sigma_{\pi}]$) represents the scaled photon energy[13] in the absence of LP's. We remind the reader that such scaling is performed in order to get rid of the different amounts of disorder in the different samples.[13]

At high enough photon energies (usually above 2–3 eV), the optical oscillator density $f_{LP\text{-}\pi}(Y_N)$ arising from the Gaussian-shaped DOS "bands" can be assumed[13] as being Gaussian-shaped itself. Hence, we can write

$$f_{LP\text{-}\pi}(Y_N)=J_{DOS\ LP\text{-}\pi}(Y_N)/Y_N\sim C\exp[-(Y_N-W_{N0})^2], \tag{12}$$

where C is a constant.

IV. THE LINEAR INTERDEPENDENCY MODEL FOR NITROGENATED FILMS

A. Introduction

In the presence of different types of transitions, at each (scaled or not) photon energy, the overall excitation coefficient ε_2 can be regarded as the sum of various contributions ($\varepsilon_2=\Sigma_i\varepsilon_{2i}$). We will neglect $\varepsilon_{2\sigma}$ as it describes transitions involving σ states ($\pi\rightarrow\sigma^*$, $\sigma\rightarrow\sigma^*$,...) and gives a small contribution in the energy range of interest. The f''_{LP} term (and, hence, ε''_{2LP}) will be disregarded as well (see above). $\varepsilon_2(Y)$ will then be the sum of the $\pi\rightarrow\pi^*$ ($=\varepsilon_{2\pi}$) and LP $\rightarrow\pi^*$ ($\sim\varepsilon'_{2LP}$) contributions $\varepsilon_2\approx\varepsilon_{2\pi}+\varepsilon'_{2LP}$. In the next sections a model useful to analyze the optical properties of slightly nitrogenated ($\sim$10%) films will be developed and its applicability will be shown to rely on the applicability of the condition $(2+\varphi)n_{CN}\gg n_{\pi}^{(0)}$.

B. The basis of the model

According to the Kramers-Krönig relations,[16] the total dielectric susceptivity (ε_1-1) can be obtained by summing the contributions related to the various transitions: $\varepsilon_1-1=\Sigma_i[\varepsilon_1-1]_i$. In our scheme, the overall dielectric susceptivity at any given energy is written as

$$\varepsilon_1-1\approx[\varepsilon_1-1]_{\sigma}+[\varepsilon_1-1]_{\pi}+[\varepsilon_1-1]'_{LP}-[\varepsilon_1-1]''_{LP}. \tag{13}$$

By multiplying $[\varepsilon_1-1]_{\pi}+[\varepsilon_1-1]'_{LP}$ by a factor $\varepsilon_2/(\varepsilon_{2\pi}+\varepsilon'_{LP})\sim 1$ we obtain, at each scaled energy Y_N,

$$\varepsilon_1(Y_N)\approx\left\{\frac{[\varepsilon_1(Y_N)-1]_{\pi}+[\varepsilon_1(Y_N)-1]'_{LP}}{\varepsilon_{2,\pi}(Y_N)+\varepsilon'_{2,LP}(Y_N)}\right\}\varepsilon_2(Y_N)+\varepsilon_{1,\sigma}(Y_N)-[\varepsilon_1(Y_N)-1]''_{LP}. \tag{14}$$

Hence, for *a*-CN:H films a relationship of the type

$$\varepsilon_1(Y_N)\approx S_N(Y_N,W_{N0})\varepsilon_2(Y_N)+I_N(Y_N,W_{N0}) \tag{15}$$

holds between $\varepsilon_1(Y_N)$ and $\varepsilon_2(Y_N)$.

C. The slope S_N

The slope S_N will be approximately given by the factor appearing in brackets in Eq. (14). As Kramers-Krönig relationships[17] allow us to write each contribution to susceptivity ($[\varepsilon_1-1]_i$) in terms of the corresponding optical oscillator density f_i, we have

$$S_N(Y_N)=\frac{[\varepsilon_1(Y_N)-1]_\pi+[\varepsilon_1(Y_N)-1]'_{LP}}{\varepsilon_{2,\pi}(Y_N)+\varepsilon'_{2,LP}(Y_N)}$$
$$=\frac{\int_{-\infty}^{+\infty}\frac{f_\pi(Z)+f'_{LP}(Z)}{Z^2-Y_N^2}dZ}{\frac{f_\pi(Y_N)+f'_{LP}(Y_N)}{Y_N}}. \quad (16)$$

In order to obtain a more useful expression for S, we will apply the procedure described by Eqs. (9) and (10) to the oscillator density $f_{LP\text{-}\pi}$ [Eq. (2)]:

$$f_{LP\text{-}\pi}(Y_N)=f'_{LP\text{-}\pi}(Y_N)-f''_{LP\text{-}\pi}(Y_N)$$
$$=C'\exp[-(Y_N-W_{N0})^2]$$
$$-C''\exp[-(Y_N-W_{N0})^2]. \quad (17)$$

The coefficients C' and C'' can be evaluated by using the f-sum rule. Hence $C=C'-C''=K'n_\pi-K''n_\pi^{(0)}$ and the following expressions are obtained:

$$f'_{LP\text{-}\pi}(Y)=K'n_\pi\exp[-(Y_N-W_{N0})^2],$$
$$-f''_{LP\text{-}\pi}(Y)=-K''n_\pi^{(0)}\exp[-(Y_N-W_{N0})^2]. \quad (18)$$

S_N can be evaluated by replacing $f_\pi+f_{LP}$ with $f_{LP\text{-}\pi}$ (i.e., substituting $f'_{LP\text{-}\pi}$ for $f_\pi+f'_{LP}$ and $f''_{LP\text{-}\pi}$ for f''_{LP}) in Eq. (16) and taking into account Eq. (12). The energy trend of the slope S_N is consequently given by

$$S_N(Y_N,W_{N0})=i\,\mathrm{erf}[i(W_{N0}-Y_N)]$$
$$+i\exp(-4W_{N0}Y_N)\mathrm{erf}[i(W_{N0}+Y_N)], \quad (19)$$

where W_{N0} represents a properly averaged value of the W_N values of the different films taken into account in a specific analysis. The possibility to use a single W value is related to the fact that the n_π dependency of the term $f_\pi+f'_{LP}$, as it affects both the numerator and the denominator in Eq. (19), cancels out. Hence, $S_N(Y)$ values do not depend on n_π (i.e., they are not affected by film features such as cluster sizes, and C sp^3, N, and H contents, etc.).

Equation (19) closely resembles the result obtained for non-nitrogenated films.[13] However, it has to be noted that the parameters involved in Eq. (16) have a different physical meaning than those involved in the ''non-nitrogenated'' case.

D. The intercept I_N

The analysis of Eq. (14) shows that the intercept can be written as

$$I_N(Y_N)=\varepsilon_{1,\sigma}(Y_N)-[\varepsilon_1(Y_N)-1]''_{LP}. \quad (20)$$

Although f''_{LP} gives a nearly negligible contribution to the overall oscillator densities, it gives a non-negligible one to the total susceptivity through the $[\varepsilon_1(Y)-1]''_{LP}$ term. In fact, at those scaled energies at which $[\varepsilon_1(Y)-1]_\sigma$ gives a weak contribution, even the small $[\varepsilon_1(Y)-1]''_{LP}$ component has its relevance in determining the intercept values I_N. The f''_{LP} related contributions will then become relevant at low Y values. Following Eqs. (20) and (10) we can write

$$I_N(Y_N)=I_0(Y_N)-\int_{-\infty}^{+\infty}\frac{f''_{LP}(Z)}{Z^2-Y_N^2}dZ. \quad (21)$$

When only the effect of σ-state related transitions is considered, I_0 can be written, by means of the Kramers-Krönig relationship and a Wemple-diDomenico model,[18] as[13]

$$I_0(Y,X_0,X_2)=1+1/(X_0-X_2Y^2), \quad (22)$$

where X_0 and X_2 are values determined by the σ related transitions. The $[\varepsilon_1(Y)-1]''_{LP}$ term accounts for the departure between the experimental (see below) and modeled [Eq. (15)] trends at low Y_N values. Indeed, as $[\varepsilon_1(Y'_N)-1]''_{LP}$ is proportional to $n_\pi^{(0)}$ and different ''a-C:H precursors'' can exist, the intercept value I_N is not unique but is affected by a certain fluctuation $\Delta I(Y)$, depending on the actual concentration $n_\pi^{(0)}$ of $\pi\rightarrow\pi^*$ oscillators in the ''a-C:H precursor.''

E. Summary

The linear interdependency model contemplates that, at each scaled energy Y_N, samples place themselves along parallel lines having $S_{N0}(W_N)$ slopes. The line on which a given a-CN:H film is actually placed (Fig. 3) depends on its ''a-C:H precursor.''

V. EXPERIMENTAL RESULTS AND DATA ANALYSIS

A. Overview

The ellipsometry data analyzed using the Tauc-Lorentz model provide the optical parameters usually selected to compare carbon-based thin films with literature data. In this study, the optical gap E_g of sputtered carbon nitrides ranges from 0.6 to 1.2 eV, and the refractive index at 2 eV is in the range 1.80–1.95 showing their graphiticlike structure. In the following, a more detailed ellipsometric model is developed in the frame of the scaling law exposed in the previous section.

Let us first focus on the energy dependence of ε_1 and ε_2 reported in Fig. 2. The analysis of the figure shows that the gross features of the optical properties of a-CN:H in the VIS-NUV range appear to be close to those of a-C:H films. However, the trends for a-C(:H) films are steeper than those of our a-CN:H films.

As a first step, we have analyzed the ε_2 energy dependence for each sample by means of the formulas reported in the Appendix. This allows to determine the values of the various parameters needed for the σ scaling, i.e., bandwidths and peak positions. Moreover, values of V_N and W_N will be obtained for each sample (see Table II).

At this stage, the σ scaling of the photon energy (i.e., the determination of the Y_N values) can be performed for each film. This allows to plot (Fig. 3), at any given Y_N, ε_1 as a

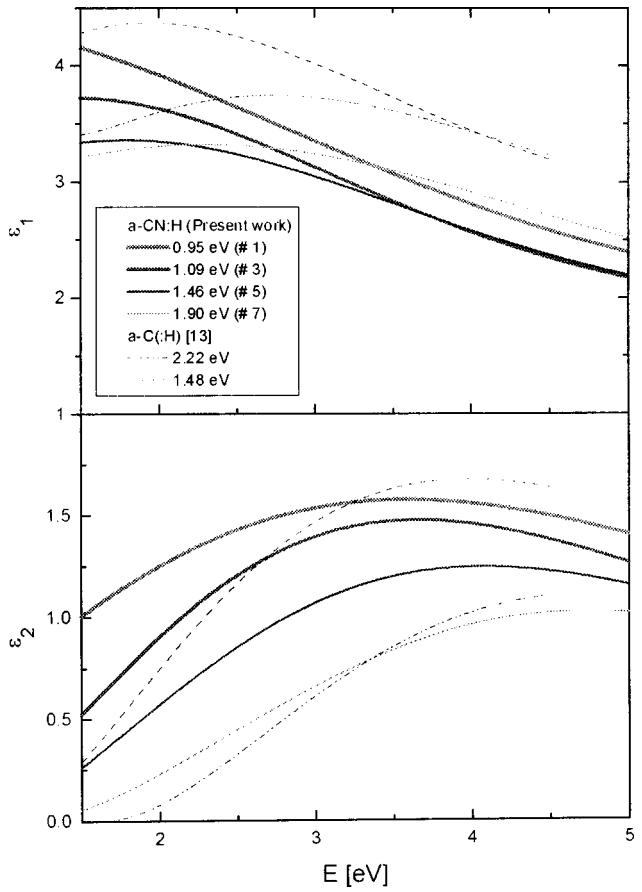

FIG. 2. Trends of the real (ε_1) and imaginary (ε_2) parts of the complex dielectric constants vs incident photon energies. Trends exhibited by samples 2, 4, and 6 are not reported since they are very close to that exhibited by sample 3. The behavior of two a-C(:H) samples (Ref. 13) is reported as well. Values in eV indicate the E_{04} gap.

function of ε_2 for all samples. A linear relationship properly describes the data at all σ-scaled energies:

$$\varepsilon_{1j}(Y_N) = S_N(Y_N)\varepsilon_{2j}(Y_N) + I_N(Y_N), \tag{23}$$

where j stands for any given sample.

The Y_N dependence of the slope S_N and the intercept I_N for our a-CN:H films (S_N and I_N in the following) are reported in Figs. 4 and 5, respectively. The lines obtained by best fitting the data with Eqs. (19) and (22) are reported as well. It can be observed that

(i) Eq. (23) (i.e., the linear interdependency model) is reasonably obeyed by the experimental curves;

(ii) the value of the average scaled peak energy obtained from the best-fit procedure ($W_{N0}=1.9$) is close to the average of the W_N values obtained from the analysis of ε_2 for each film (see Table II);

(iii) departures from the linear interdependency model occur in samples having E_{04} values well below ~1.1 eV. Such a behavior is in fact clear only for the sp^2-rich sample 1 (Fig. 3) having $E_{04}\sim 0.95$ eV.

TABLE II. Optical and DOS parameters of the films (see text for the meaning of the symbols).

Sample	1	2	3	4	5	6	7
Tauc gap E_g (eV)	0.58	0.68	0.71	0.73	0.84	0.88	1.14
E_{04} gap (eV)	0.95	1.20	1.09	1.18	1.46	1.34	1.90
E_π^* (eV)	1.63	1.68	1.71	1.73	1.95	1.77	2.44
$P_{\pi N}=E_\pi^*+E_{\pi N}$ (eV)	4.06	3.99	4.11	4.04	4.52	3.94	5.00
σ_π (eV)	0.68	0.70	0.72	0.73	0.82	0.74	1.02
$\sigma_{\pi N}$ (eV)	1.22	1.12	1.18	1.11	1.24	1.01	1.15
V_N	1.22	1.13	1.17	1.10	1.00	1.10	0.83
W_N	1.66	1.79	1.74	1.82	1.83	1.95	2.17

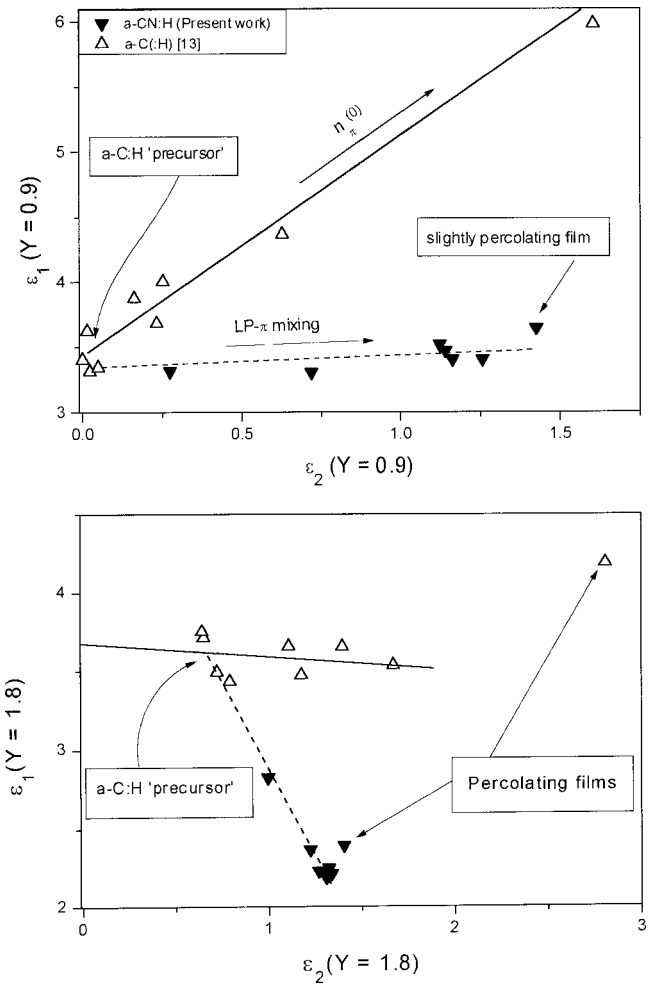

FIG. 3. Linear interdependency of the optical constants ε_1 and ε_2 at two different scaled energies: (a) $Y=0.9$; (b) $Y=1.8$. Two percolating (a-C:H and a-CN:H) samples with different threshold values are shown. The effects of LP-π mixing and LP delocalization (see text) are sketched.

Analyzing the data in Fig. 5 by Eq. (22), the values of X_0 (=0.529) and X_2 (=0.035) can be extracted. A detailed discussion of these parameters is, however, beyond the scope of this paper.

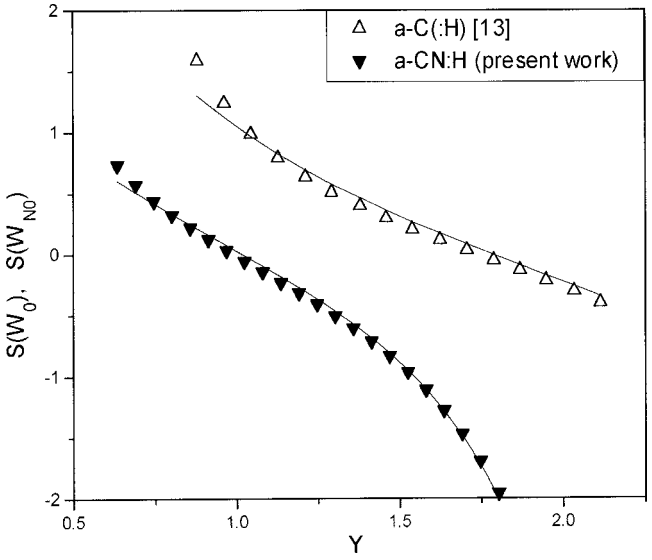

FIG. 4. Slopes of the ε_1 vs ε_2 linear relationships for a-CN:H and a-C:H. Lines represents the fitting obtained with Eq. (19).

B. Looking for information about LP and their mixing with π states

The values of V_N ($=E_{LP}/E_\pi$) reported in Table II vary in the range 0.8–1.2. Hence, the peaks of LP and π states are quite close in energy and this favors their mixing. Since the two peaks are so close in energy, the main effect of mixing will be to broaden the bonding state DOS, leaving almost unchanged the energy spacing between (π-LP mixed) bonding and (π^*) antibonding band peaks.

The high E_{LP} values (of the order of E_π, i.e., 2–3 eV) confirm that the LP states are strongly stabilized by the environment. Such stabilization can be attributed to the medium-range polarization and interactions related to the charge transfer occurring in the sp^2 carbon phase because of the nitrogenated inclusions.[11] Actually, in the considered a-CN:H samples it is expected that the medium-range polarization of the π states creates regions of the carbon phase where the electronic charge density is lower. Such regions will conjugate with the LP electrons and stabilize the nitrogen-related lone-pair states. It must be noted that a-CN:H films cannot be simply regarded as a collection of "molecules," since disorder and medium-range interaction among the various groups and clusters strongly affect their properties.

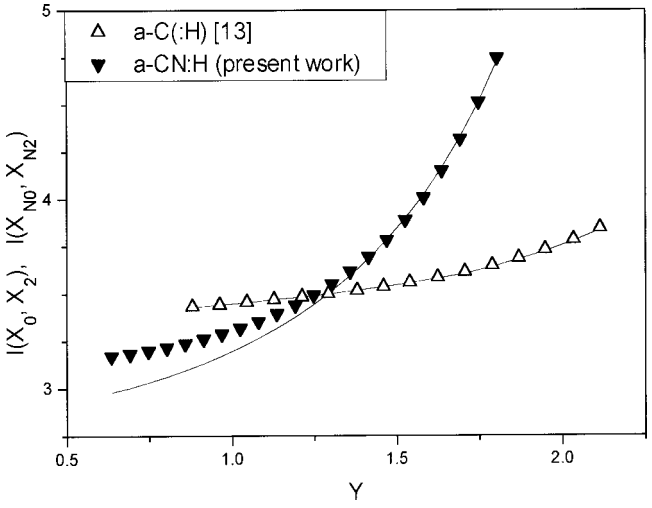

FIG. 5. Scaled energy dependence of the intercept of the linear interdependency relationship for a-CN:H. The line is obtained by best fitting the $1/(I_0-1)$ trends (linear in Y) from Eq. (22).

In order to further investigate the role of LP-π mixing, it is interesting to compare the results obtained for a-CN:H films with those obtained in the a-C:H case.[13] The existence of a linear relationship between ε_1 and ε_2 at any given σ-scaled energy allows in fact a quantitative understanding on a common basis of the DOS features of a-C:H or a-CN:H films. However, the various parameters (W, X_0, X_2, and subsequently S, I, . . .) have different values and physical meanings for a-C:H and a-CN:H films.

In the case of a-CN:H the S_N (and I_N) vs Y curves are less steep (see Figs. 4 and 5). The lower values of slope are due to the more relevant role played by the σ-π mixing as a consequence of the presence of the σ-like LP states. The bonding DOS "band" broadens ($\sigma_{LP\text{-}\pi} > \sigma_\pi$) because of the LP-$\pi$ mixing effect. Such an effect increases the bandwidth $\sigma_{\pi N}$ of the joint density of states and the optical oscillator density [Eq. (12)]. Finally, W_{N0} will be lower than the corresponding W_0 [=2.4 (Ref. 13)] value. As the peak-to-peak energy spacing is similar, this amounts to having wider Gaussian "bands" in a-CN:H and is a consequence (see above) of the LP-π mixing.

While departures from the linear interdependency model occur in a-C(:H) samples having $E_{04} \sim 1.3$ eV, such a model still holds for a-CN:H films having $E_{04} \sim 1.1$ eV. It has been argued[13] that the departure from the linear behavior in the $\varepsilon_1(Y)$ vs $\varepsilon_2(Y)$ plot is related to the onset of percolation for (i.e., the formation of extended) π and π^* states, which occurs in a-C:H films having low E_{04} [<1.3 eV; i.e., sp^2 >80% (Ref. 13)]. When percolation occurs (i.e., for Y exceeding a threshold scaled energy Y_{pt}) Eq. (23) no longer holds. In a-CN:H samples Eq. (23) still holds for films with E_{04} values well below the threshold value in a-C:H films. This suggests that in the presence of nitrogen a higher sp^2 content is required to render π states percolating, despite the broader absorption band tails of nitrogenated films. This indicates the important role of LP states that, by mixing with π states, leads to mixed LP-π states more localized than the original (unmixed) π ones.

Of course, the presence of a relevant sp^1 phase might partially modify the shape of the π DOS since each sp^1 site involves two π electrons occupying two degenerate states. However, at a given number of π electrons per unit volume, films having a higher sp^1/sp^2 ratio would also have a π-electron distribution more localized around sp^1 sites. Moreover, degenerate electronic states have the same energy and the sp^1 phase is expected to increase the network floppiness. We would then expect a shrinking rather than a broadening of π- and π^*-DOS bands. Finally, in presence of a π-DOS perturbation mainly caused by the direct effect of the sp^1 phase, the linear relationship between ε_1 and ε_2 [Eq.

(3)] would vanish since their relationship will be determined by the actual sp^1/sp^2 ratio of each sample. This facts suggest that π states related to sp^1 sites have a limited role in determining the optical properties of our *a*-CN:H films.

VI. CONCLUDING REMARKS

We have shown that the optical properties of a set of *a*-CN:H thin films having quite different physical properties can be described on a common basis. The crucial role played by the nitrogen atoms in promoting either directly (sp^1 hybrids involving one more π electron than sp^2 hybrids) or indirectly (sp^1 hybrids inducing carbon sp^2 island nucleation around them) the increase of the π-electron density was discussed.

The lone pairs belonging to the nitrogen atoms are of crucial importance in determining the optical properties of the films. LP states can mix either with other *atomic* orbitals of the same N atom or with the *molecular* π orbitals formed by the clustered C and/or N atoms surrounding the lone pair. As a consequence, a single ''valence'' LP-π band of localized states is formed and transitions occur to the states of the π^* band. Assuming such bands to have quasi-Gaussian shapes, the absorption properties in the energy range close to the Gaussian peak-to-peak energy spacing have been properly modeled.

On the basis of such an approach, the existence of a linear interdependency between causally related optical constants and the differences of the involved parameters with respect to the *a*-C:H case[13] have been justified. The existence of a common ''*a*-C:H precursor'' for the set of *a*-CN:H films, with a common concentration of π-π^* oscillators, has been proposed.

APPENDIX: JOINT DENSITY OF STATES IN THE PRESENCE OF LP-π MIXING AND LP DELOCALIZATION

In Sec. III B we have justified the assumption that the density of LP, π, and π^* states are described by Gaussian-shaped disorder-broadened bands centered at $-E_{\mathrm{LP}}$, $-E_{\pi}$, and E_{π^*}, respectively. We have also demonstrated the validity of the following assumption:

$$E_{\pi}/\sigma_{\pi}=E_{\pi^*}/\sigma_{\pi^*}=E_{\mathrm{LP}}/\sigma_{\mathrm{LP}}=W_0=\text{const.}$$

Under negligible LP-π mixing conditions, the Gaussian-shaped π and π^* DOS can be written in terms of the scaled photon energy Y ($=E/[2\sigma_x]$) and the scaled peak-to-peak spacing W_0 ($=E_{\pi}/[\sigma_{\pi}]$):

$$N_i(Y,W_0)=N_{i,\max}\exp[-(Y\pm W_0/2)^2], \tag{A1}$$

where $+$ holds for $i=\pi$ (i.e., bonding DOS) and $-$ for $i=\pi^*$ (i.e., antibonding DOS).

The Gaussian-broadened LP DOS can be written in terms of Y and W_0:

$$N_{\mathrm{LP}}\left(\frac{Y}{V_{\mathrm{N0}}},-W_0\right)=N_{\mathrm{LP,max}}\exp\left[-\frac{(E+E_{\mathrm{LP}})^2}{2\cdot\sigma_{\mathrm{LP}}^2}\right]=N_{\mathrm{LP,max}}\exp\left[-\left(\frac{Y}{V_{\mathrm{N0}}}+\frac{W_0}{2}\right)^2\right], \tag{A2}$$

where a further dimensionless parameter

$$V_{\mathrm{N0}}=E_{\mathrm{LP}}/E_{\pi}=\sigma_{\mathrm{LP}}/\sigma_{\pi}$$

takes into account the peak position E_{LP} (and the bandwidth σ_{LP}) of the LP DOS. For LP states sitting on the average nonbonding level we have $V_{\mathrm{N0}}=0$ and a δ-shaped LP DOS, while $V_{\mathrm{N0}}=1$ implies that the π and LP DOS are superposed.

Let us suppose that a full LP-π mixing occurs without any relevant energy gain. This is a reasonable assumption as the two states merge in order to prevent the energy loss that the local distortions would impose on nonmixed states. The density of bonding states obtained by mixing the whole π DOS and the whole LP DOS will be given by the convolution product of the two bands

$$N_{\mathrm{LP}\text{-}\pi}(Y)=\int_{-\infty}^{+\infty}N_{\mathrm{LP}}\left(\frac{Y-Z}{V_{\mathrm{N0}}},-W_0\right)N_{\pi}(Z,-W_0)dZ=N_{\mathrm{LP}\text{-}\pi,\max}\exp\left\{-\frac{[4Y+W_0(1+V_{\mathrm{N0}})]^2}{8(V_{\mathrm{N0}}^2+1)}\right\}. \tag{A3}$$

The result is the formation of a LP-π mixed DOS band located at an intermediate energy and wider than each of its components. The joint density of states (J_{DOS}) will be obtained by properly convoluting the density of occupied states with the density of unoccupied ones. Considering only the (π-LP)$\rightarrow\pi^*$ transition,

$$\begin{aligned}J_{\mathrm{DOS,LP}\text{-}\pi}(Y)&=\int_0^Y N_{\mathrm{LP}\text{-}\pi}(Z-Y)N_{\pi}^*(Z)dZ\\&=C''\exp\left\{-\frac{[4Y-W_0(V_{\mathrm{N0}}+3)]^2}{8\cdot(2+V_{\mathrm{N0}}^2)}\right\}\\&\quad\times\left\{\mathrm{erf}\left[\frac{4Y+W_0(2V_{\mathrm{N0}}^2-V_{\mathrm{N0}}+1)}{2[2(V_{\mathrm{N0}}^2+1)(V_{\mathrm{N0}}^2+2)]^{1/2}}\right]\right.\\&\quad\left.-\mathrm{erf}\left[\frac{-4Y(1+V_{\mathrm{N0}}^2)+W_0(2V_{\mathrm{N0}}^2-V_{\mathrm{N0}}+1)}{2[2(V_{\mathrm{N0}}^2+1)(V_{\mathrm{N0}}^2+2)]^{1/2}}\right]\right\}.\end{aligned} \tag{A4}$$

As the term inside brackets has a quasilinear Y dependence in the region of interest, the optical oscillator densities $f_{\mathrm{LP}\text{-}\pi}(Y)$

$[=J_{\mathrm{DOS,LP}\text{-}\pi}(Y)/Y]$ is approximately Gaussian shaped.[13] In particular, if we introduce a new scaled photon energy

$$Y_{\mathrm{N}}=\frac{2}{[2(V_{\mathrm{N0}}^2+2)]^{1/2}}Y\leqslant Y$$

and a new scaled peak-to-peak energy

$$W_{\mathrm{N0}}=\frac{V_{\mathrm{N0}}+3}{2[2(V_{\mathrm{N0}}^2+2)]^{1/2}}W_0 \tag{A5}$$

we can write

$$f_{\mathrm{LP}\text{-}\pi}(Y_{\mathrm{N}})=J_{\mathrm{DOS,LP}\text{-}\pi}(Y)/Y\sim C\exp[-(Y_{\mathrm{N}}-W_{\mathrm{N0}})^2]$$

(where $C\neq C''$). It has to be noted that the new energy scale (Y_{N}) differs from the original one (Y) for $V_{\mathrm{N0}}>0$, as it will be $Y_{\mathrm{N}}=Y$ only for $V_{\mathrm{N0}}=0$ (i.e., in the absence of lone-pair stabilization by the environment).

Equation (A5) is crucial, since it links the values of the scaled peak-to-peak energy in the absence of LP-π mixing and in the presence of a complete LP-π mixing. For nonstabilized (i.e., nonmixed) lone pairs ($V_{\mathrm{N0}}=0$). $W_{\mathrm{N0}}=3W_0/4$, while in the presence of high stabilization ($V_{\mathrm{N0}}=1$, i.e. LP states sitting at the same energy of π-bonded states), it will be $W_{\mathrm{N0}}=\sqrt{2/3}W_0$.

*Present address: Opsys Ltd., Begbroke Business and Science Park, Yarnton, Oxford OX5 1PB, UK.

[1] S. Muhl and J. M. Mendez, Diamond Relat. Mater. **8**, 1809 (1999), and references therein.
[2] S. Bhattacharyya, C. Cardinaud, and G. Turban, J. Appl. Phys. **83**, 4491 (1998).
[3] M. Zhang, Y. Nakayama, and M. Kume, Solid State Commun. **110**, 679 (1999).
[4] J. Wagner and P. Lautenschlager, J. Appl. Phys. **59**, 2044 (1986).
[5] M. Chhowalla, R. A. Aharanov, C. J. Kiely, I. Alexandrou, and G. A. J. Amaratunga, Philos. Mag. Lett. **75**, 329 (1997).
[6] A. Ilie, O. Harel, N. M. J. Conway, T. Yagi, J. Robertson, and W. I. Milne, J. Appl. Phys. **87**, 789 (2000).
[7] B. Kleinsorge, A. C. Ferrari, J. Robertson, and W. I. Milne, J. Appl. Phys. **88**, 1149 (2000).
[8] F. Demichelis, G. Giachello, C. F. Pirri, A. Tagliaferro, and E. Tresso, SPIE, Diamond Optics IV **1534**, 140 (1991).
[9] G. Fanchini, A. Tagliaferro, G. Messina, S. Santangelo, A. Paoletti, and A. Tucciarone, J. Appl. Phys. **91**, 1155 (2002).
[10] R. M. A. Azzam and N. M. Bashara, *Ellipsometry and Polarized Light* (Elsevier, Amsterdam, 1987).
[11] G. Fanchini, G. Messina, A. Paoletti, S. C. Ray, S. Santangelo, A. Tagliaferro, and A. Tucciarone, Surf. Coat. Technol. **151–152**, 257 (2002).
[12] G. Fanchini, A. Tagliaferro, D. P. Dowling, K. Donnelly, M. L. McConnell, R. Flood, and G. Lang, Diamond Relat. Mater. **9**, 732 (2000).
[13] G. Fanchini, A. Tagliaferro, D. P. Dowling, K. Donnelly, M. L. McConnell, R. Flood, and G. Lang, Phys. Rev. B **61**, 5002 (2000).
[14] H. Efstathiadis, Z. Akkermann, and F. W. Smith, J. Appl. Phys. **79**, 2954 (1996).
[15] G. Fanchini and A. Tagliaferro, Diamond Relat. Mater. **10**, 191 (2001).
[16] G. D. Cody, in *Hydrogenated Amorphous Silicon, Semiconductors and Semimetals*, edited by J. J. Pankove (Academic, New York, 1984), Vol. 21B, p. 11.
[17] D. Y. Smith, in *Handbook of Optical Constants of Solids*, edited by E. D. Pawlik (Academic, New York, 1985), pp. 38–47.
[18] S. H. Wemple and M. diDomenico, Phys. Rev. B **3**, 1338 (1971).